Angular-dependent *I–V* characteristics in borocarbide superconductor YNi_2B_2C

2006 J. Phys.: Condens. Matter 18 4085

(http://iopscience.iop.org/0953-8984/18/16/015)

INSTITUTE OF PHYSICS PUBLISHING JOURNAL OF PHYSICS: CONDENSED MATTER

J. Phys.: Condens. Matter **18** (2006) 4085–4092 doi:10.1088/0953-8984/18/16/015

Angular-dependent I–V characteristics in borocarbide superconductor YNi_2B_2C

R M Chu[1,4], Q Y Chen[2] and W K Chu[2,3]

[1] Bio-Nano Computational Laboratory (RCMI-NCRR) and Physics Department, Texas Southern University, Houston, TX 77004, USA
[2] Texas Center for Superconductivity at University of Houston (T_CSUH), Houston, TX 77204-5002, USA
[3] Physics Department, University of Houston, Houston, TX 77204-5005, USA

E-mail: chu_rk@tsu.edu

Received 15 September 2005, in final form 19 March 2006
Published 7 April 2006
Online at stacks.iop.org/JPhysCM/18/4085

Abstract

We present angular-dependent current–voltage (I–V) measurements in borocarbide YNi_2B_2C single crystals near the vortex-glass irreversible line. External magnetic fields are applied along the angle θ with respect to the c-axis. The nonlinear I–V curves reveal scaling behaviour near the transition. Using the scaling analysis, the relevant critical exponents and vortex transition temperatures are determined for all orientations. The data agrees well with the vortex-glass (VG) model. No evidence was found that supports the existence of a Bose-glass (BG) type of transition.

1. Introduction

The discovery [1, 2] of superconductivity in intermetallic borocarbide superconductors RTM_2B_2C (R = Lu, Y, Dy, Er, Ho, or Tm, TM = Ni, Pd, or Pt) has generated much excitement because of their relatively high transition temperatures and the successful synthesis of large, high-quality single crystals. Most surprisingly, both superconductivity and long-range magnetic order coexist in the magnetic members of these compounds at low temperatures [3, 4]. This opens up the possibility of exploring the interplay between superconducting and antiferromagnetic ordering and suggests that exotic pairing mechanisms and unusual mixed states properties could exist. Interestingly, an anomalous sign-reversal of the magnetoresistance has been reported in the normal state of nonmagnetic YNi_2B_2C single crystals. The quenching of local magnetic ordering and perhaps inducted spin fluctuations might explain this observation [5].

[4] Author to whom any correspondence should be addressed.

Borocarbide superconductors, which are believed to be conventional type-II superconductors with s-wave symmetry, have recently attracted renewed attention because of strong evidence of the existence of a highly anisotropic superconducting gap. The symmetry of the order parameter has been examined extensively by various experimental probes, such as specific heat [6, 7], photoemission spectroscopy [8], microwave impedance [9], scanning tunnelling microscopy [10], ultrasonic attenuation [11], and point-contact spectroscopy [12]. In addition, the transport and rf (radio frequency) penetration depth measurements of YNi_2B_2C [13] derive a complicated HT-phase diagram, which separates the non-dissipative vortex solid from the resistive vortex liquid. It was also found that, when $H \geqslant 2$ T, the vortex lattice undergoes a continuous transition into the vortex-glass phase [14], as observed in high-temperature superconductors [16, 15].

Furthermore, in RTM_2B_2C (R = Lu, Y), the Ginzburg–Landau parameter $\kappa > 6$, the Ginzburg number which measures the order of thermal fluctuation $G_i \sim 10^{-7}$, and an upper critical field B_{c2} as high as 10 T, the mixed state and the role of pinning disorders of YNi_2B_2C could therefore be quite unusual compared with conventional superconductors and high-temperature superconductors (HTS). In fact, the anisotropy of the vortex lattice and transition have been imaged by STM [10, 17]. In order to shed light on the possible role of the correlated disorders in this compound, we present the angular-dependent I–V transport measurements near the solid–liquid transition in YNi_2B_2C single crystals as a function of the temperature and tilting angle between the applied magnetic field and the c-axis. The scaling analysis results are consistent with the vortex-glass (VG) transition. In addition, the experiments allow the determination of VG transition temperature T_g and static and dynamic critical exponents ν and z with respect to all orientations.

2. Experimental details

A rod-like large single crystal of YNi_2B_2C was grown by the zone-refining method with arc-melted polycrystalline stoichiometric ingots used as the seed [18]. The dimensions of the grown single-crystalline rod were about 80 mm long and 6 mm in diameter. X-ray diffraction patterns showed that the crystal was homogeneous, without any trace of a secondary phase. DC magnetization measurements determined the superconducting transition temperature, $T_c = 15.3$ K, with a transition width of less than 500 mK. In addition, the H_{c2} parallel to the [100] and [001] directions were 7 T and 6 T at 4.2 K. The residual resistivity ratio $\rho(300\text{ K})/\rho(20\text{ K}) = 11$ indicates that the sample is in the clean limit [7]. The orientations and structure perfection were examined by Rutherford backscattering (RBS) ion-beam channelling performed at room temperature using the 1.7 MeV Tandem accelerator facility (Model 5SDH-2 by National Electrostatics Corp.) located at the Texas Center for Superconductivity at the University of Houston. The measurements were performed on the [001] surfaces of YNi_2B_2C single crystals. Figure 1 shows 1.5 MeV $^4He^+$ RBS-channelling spectra for random and [001]-aligned directions. Y and Ni backscattered signals can be clearly identified because of their relatively heavy atomic mass. Likewise, it is impossible to distinguish B and C signals from the background because of their relatively light atomic mass and thus low scattering cross section. The normalized minimum yield, χ_{min}, is defined as the ratio of the backscattered counts in a narrow energy window (usually set near the crystal surface) between the aligned (channeled) and random spectra [19]. In the [001] samples near the surface, χ_{min} approximately equals 3%, demonstrating the high degree of crystallinity of the samples.

To prepare for the I–V transport measurements, the crystal was cut into several rectangular parallelepipeds. The dimensions of the samples were approximately 0.5 mm × 0.5 mm × 4 mm. Surface pinning was minimized by chemical etching the

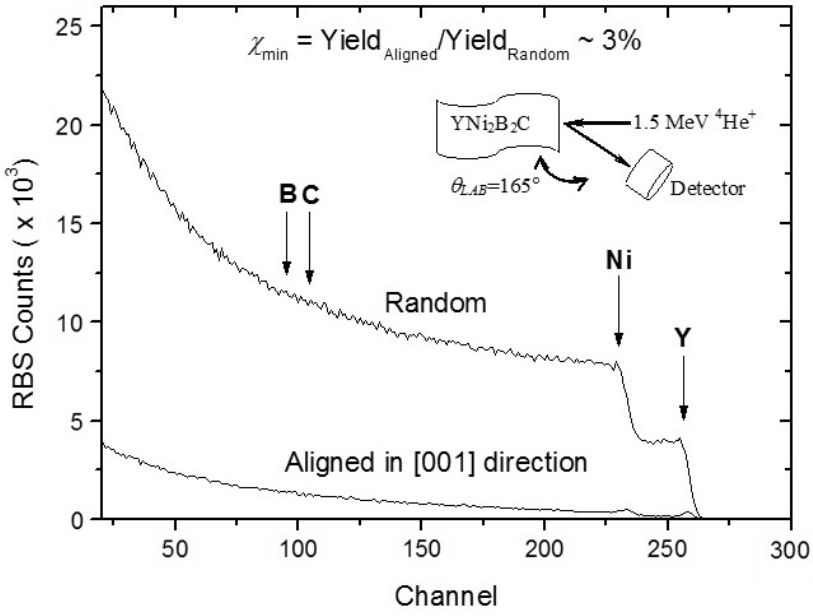

Figure 1. 1.5 MeV $^4He^+$ RBS-channelling spectra of c-axis YNi_2B_2C single crystal. Yield$_{Aligned}$ and Yield$_{Random}$ are the backscattered yields in the aligned (001) direction and in the random direction, respectively.

specimens in a 3-to-1 solution of HCl–HNO_3 [20]. The sample was mounted onto a rotatable sample holder with an angular resolution of 0.05° inside a cryostat in an 8 T external magnetic field. In all measurements, the fields were applied to the sample above T_c before cooling down the sample. The ac voltages were measured as a function of temperature by a lock-in amplifier at 30 Hz. For the resistivity and I–V measurements, current densities $J \leqslant 2.5$ A cm^{-2} were applied through the crystal perpendicular to the ac plane. The rotation of the magnetic field off the a-axis was performed at constant Lorentz force for fields between 1 T and 8 T. The multicriticality of the vortex lattice/glass phase has been observed in the crossover low-field region of 1 T $\leqslant H \leqslant$ 2 T in the YNi_2B_2C single crystal [14]. In order to avoid inconclusive results, we preform our measurements close to the VG region with $H = 3$ T. The applied voltage resolution of the measurements is about 100 pV (HP34420A nanovoltmeter).

3. Results and discussion

Since the effective pinning strength of the disorder is proportional to the field intensity [15], the unstable vortex lattice will form a glass phase. The properties of the system in the region of the phase diagram surrounding the phase boundary are dominated by fluctuations. In this critical region, the dynamical response of the vortex lattice can be obtained through a critical scaling theory by equating the appropriate dimensionless quantities [16, 15]. In particular, the relation between the current density J and electric field E when the magnetic field is aligned with the defects obeys [16, 15]:

$$\frac{E}{J\left|T - T_g\right|^{\nu(z-1)}} = F_{\pm}\left(\frac{J}{T\left|T - T_g\right|^{2\nu}}\right), \tag{1}$$

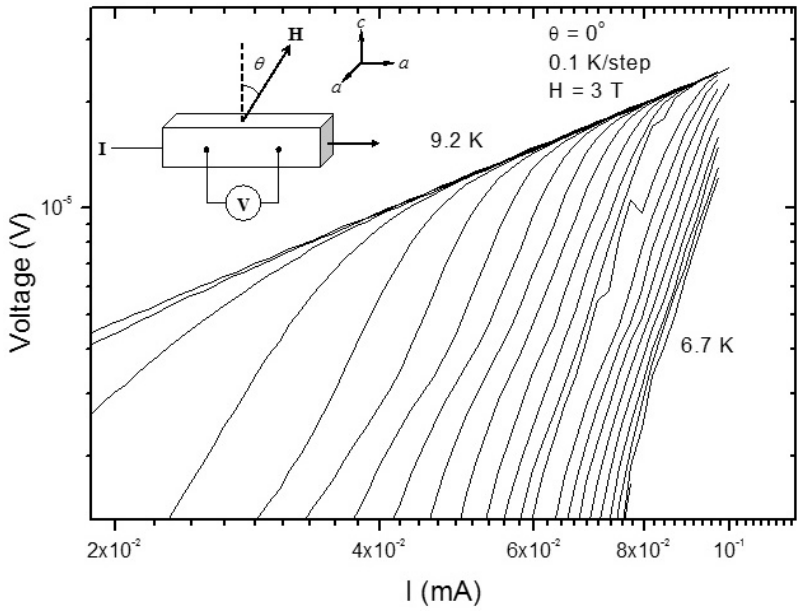

Figure 2. Log–log plot of I–V curves at $H = 3$ T and $\theta = 0°$ for selected temperatures from 6.7 K to 9.2 K with 0.1 K/step. At each temperature, a high and low current-sweet I–V curve was measured and spliced together at 20 μV. The change of sample temperature will result in curvatures difference between the upper and lower I–V curves.

where ν and z are the exponents governing the size and time relaxation of fluctuations, respectively, T_g is the vortex-glass transition temperature, and $F_\pm$ are two analytic functions for $T - T_g > 0$ and $T - T_g < 0$, respectively.

Taking the possibility of correlated defects into account, Fisher proposed a more general vortex-glass model [24]. Nelson and Vinokur further elaborated this second-order phase transition in the presence of correlated disorders. The new anisotropic Bose-glass (BG) phase possesses somewhat different scaling behaviour to the VG model. The main difference between both models arises when the applied magnetic field is rotated off the c-axis. The Bose-glass phase predicts a different vortex melting mechanism and set of new universal exponents when the field is tilted away from the normal alignment [26]. Instead of a smooth increasing function of $T_g(\theta)$ in the VG model, a *cusp* angular dependence of the glass transition temperature (T_g) should appear on the irreversibility line [25, 26]. The critical exponents of the VG model (primed) and the BG model (un-primed) are related as

$$\begin{aligned} z' &= \tfrac{1}{2}(3z + 1) \\ \nu' &= \tfrac{2}{3}\nu. \end{aligned} \tag{2}$$

In this sense, the BG model is the generalization of the glass transition in the mixed state. Therefore, it is sufficient to determine the critical exponents by analyzing the VG model and then deriving the corresponding results from (2). In fact, this universal behaviour for the I–V characteristics has been well-studied in HTS such as YBCO [21, 22].

Figure 2 plots the I–V curves at constant temperature for $H = 3$ T and $H \parallel c$. Not shown are similar I–V data for different tilt angles, $\theta = 0°$, 15°, 45°, 60°, 75°, and 90° away from H. The orientation of the measurements is shown in the inset of figure 2. In spite of the widely adopted I–V critical scaling analysis, it is not sufficient to determine the T_g by

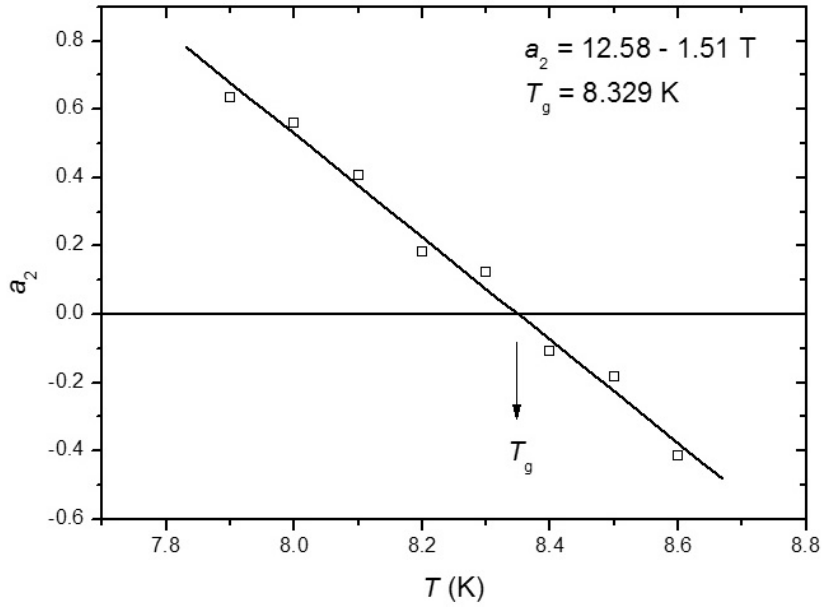

Figure 3. Using the nonlinear Levenberg–Marquardt process, a_2 of the phenomenological polynomial, $\log E = a_0 + a_1 \log J + a_2 \log^2 J$, in the vicinity of the glass transition temperature T_g, are estimated. $a_2 = 0$ represents the critical line, which divides the ohmic and non-ohmic region. The analysis is for $\theta = 0°$. Similar results were obtained for all other orientations.

Table 1. The glass transition temperatures for different rotating θ away from the field direction.

θ	0°	15°	45°	60°	75°	90°
T_g (K)	8.33	8.33	8.36	8.46	8.55	8.67

simply inspecting the set of isotherms and locating the critical line, which divides the positive curvatures (ohmic) and negative curvatures (nonlinear). Instead, consider a phenomenological second-order polynomial of the form $\log E = a_0 + a_1 \log J + a_2 \log^2 J$, where the coefficient a_2 measures the nonlinearity. Using nonlinear least-square Levenberg–Marquardt iteration [23], a_2 is obtained for every single isotherm. The glass transition temperature T_g can then be determined by plotting T against a_2, as shown in figure 3. T_g appears to be the x-intercept and is estimated to be equal to 8.33 ± 0.01 K, which is within the experimental error. From equation (1), we construct a log–log plot of $V/(I|T - T_g|)^{\nu(z-1)}$ against $I/(T|T - T_g|)^{2\nu}$; 26 isotherms from figure 2 collapse into two curves, F_+ representing the data above T_g, and F_-, representing the data below T_g. The critical exponents are $\nu = 1.27 \pm 0.01$ and $z = 5.77 \pm 0.5$.

From the same procedure repeated for $\theta = 15°$, 45°, 60°, 75°, and 90°, the set of T_g, ν, and z were evaluated. Tables 1 and 2 show the glass transition temperatures, static, and dynamical exponents for different θ tilted away from the field direction. The most striking fact is the angular dependence of T_g. The scaling *ansatz* predicted by the BG model would be that the critical angle θ_c should scale $(T_{BG} - T)^{3\nu}$ as $T \to T_{BG}$, where $T_{BG}(\theta)$ is the BG transition temperature, as shown by the dashed line in figure 4, so there would be an upward cusp in the apparent irreversibility temperature as a function of tilting angle [26, 27]. The tip of the cusp occurs when the field aligned perfectly with the correlated disorders. This is a kind of commensurate–incommensurate phase transition. As it is tilted away from the alignment,

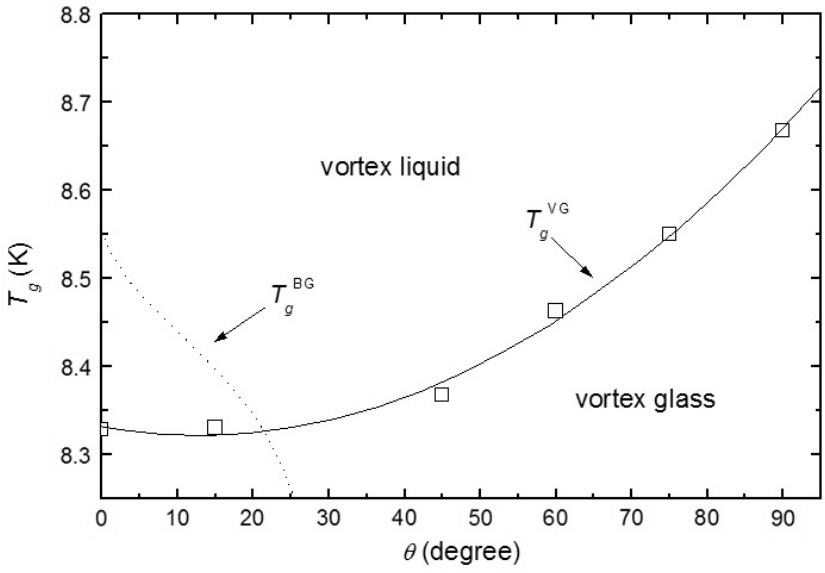

Figure 4. Angular dependence of T_g for all θ. The solid line through the data points is a guide to the eye, while the dashed line is from the prediction of the BG model (after [27]).

Table 2. Static and dynamic critical exponents for all orientations.

θ	0°	15°	45°	60°	75°	90°
ν	1.27	1.32	1.27	1.22	1.25	1.27
z	5.77	5.82	5.92	5.95	5.78	5.84

the transition will gradually evolve from BG to an anisotropic Abrikosov flux lattice, which extends far beyond both directions perpendicular to the flux line orientation [27].

However, as shown in figure 4, we find that the irreversibility line is a smooth increasing function of $T_{BG}(\theta)$, as anticipated from the VG model, and it divides the mixed state into two static phases, namely the upper vortex-liquid region and the lower vortex-glass region. Our estimated $T_{BG}(\theta = 0°)$ is consistent with the other result [14]. The static and dynamic critical exponents ν and z were adjusted accordingly for each orientation such that the optimum collapse was obtained. In figure 5, we show our results of the scaling collapse for all the orientations, and it consists of a total of 60 curves ranging from 7.9 K to 8.8 K with 0.1 K/step for $\theta = 0°, 15°, 45°, 60°, 75°$, and 90°. ν and z in table 2 are used to construct the collapse. The full scaling collapse of all data at all angles and the similarity of ν and z give strong evidence that the scaling function itself is isotropic. This indicates that the VG model better describes the intermediate transition from vortex solid to vortex liquid state in the YNi_2B_2C compound.

4. Conclusions

In summary, we have shown an extensive scaling analysis for the angular dependence of I–V data in YNi_2B_2C crystals in the vicinity of the irreversibility line, which corresponds to a second-order vortex-glass transition. Static and dynamics exponents have been extracted for all orientations with respect to the field direction. The proportionality of the glass transition

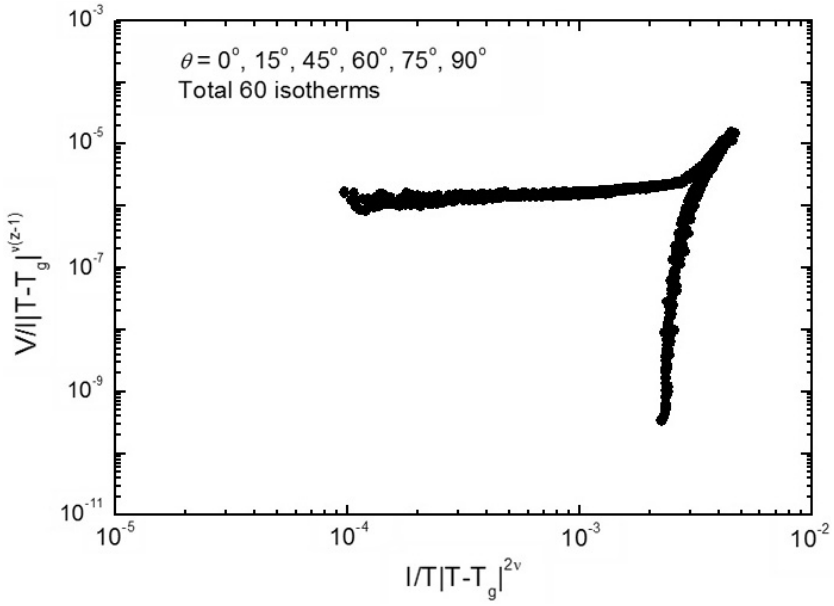

Figure 5. Scaling collapse of voltage–current curves for all rotating angles for $H = 3$ T at temperatures from 7.9 K to 8.8 K in steps of 0.1 K. The critical exponents used here are shown in table 2.

temperature to the tilt angle and the full scaling collapse provides experimental evidence for the existence of the vortex-glass phase.

Acknowledgments

We thank Hidenori Takeya for providing high-quality YNi_2B_2C samples. We are very grateful to Z H Zhang, who assisted us with the RBS-channelling experiment, and to J R Claycomb for stimulating discussions and reviewing our manuscript. This work was supported, in part, by RCMI through NIH-NCRR (G12-RR-03045), Texas Southern University Research Seed Grant 2004/2005, the State of Texas through the Texas Center for Superconductivity at University of Houston, and the US National Science Foundation Grant DMR-0404542.

References

[1] Cava R J *et al* 1994 *Nature* **367** 146
[2] Nagarajan R *et al* 1994 *Phys. Rev. Lett.* **72** 274
[3] Lynn J W *et al* 1997 *Phys. Rev.* B **55** 6584
[4] Canfield P C, Gammel P L and Bishop D J 1998 *Phys. Today* **51** (10) 40
[5] Chu R K, Chu W K, Chen Q, Zhang Z H and Miller J H Jr 2000 *J. Phys.: Condens. Matter* **12** 275
[6] Nohara M, Isshiki M, Sakai F and Takagi H 1999 *J. Phys. Soc. Japan* **68** 1078
[7] Nohara M, Suzuki H, Mangkorntong N and Takagi H 2000 *Physica* C **341–348** 2177
[8] Yokoya T, Kiss T, Watanabe T, Shin S, Nohara M, Takagi H and Oguchi T 2000 *Phys. Rev. Lett.* **85** 4952
[9] Takaki K *et al* 2002 *Phys. Rev.* B **66** 184511
[10] Martinez-Samper P, Suderow H, Vieira S, Brison J P, Luchier N, Lejay P and Canfield P C 2003 *Phys. Rev.* B **67** 14526
[11] Watanabe T, Nohara M, Hanaguri T and Takeya H 2004 *Phys. Rev. Lett.* **92** 147002

[12] Raychaudhuri P, Jaiswal-Nagar D, Sheet G, Ramakrishnan S and Takeya H 2004 *Phys. Rev. Lett.* **93** 156802
[13] Oxx S, Choudhury D P, Willemsen B A, Srikanth H, Cho B K, Canfield P C and Sridhar S 1996 *Physica* C **264** 103
[14] Mun M O, Lee S I, Lee W C, Canfield P C, Cho B K and Johnston D C 1996 *Phys. Rev. Lett.* **76** 2790
[15] Fisher D S, Fisher M P A and Huse D A 1991 *Phys. Rev.* B **43** 130
[16] Fisher M P A 1989 *Phys. Rev. Lett.* **62** 1415
[17] Sakata H, Oosawa M, Matsuba K, Nishida N, Takagi H and Hirati K 2000 *Phys. Rev. Lett.* **84** 1583
[18] Takeya H, Hirano T and Kadowaki K 1996 *Physica* C **256** 220
[19] Chu W K, Mayer J W and Nicolet Marc A 1978 *Backscattering Spectrometry* (New York: Academic)
[20] De Wilde Y *et al* 1997 *Phys. Rev. Lett.* **78** 4273
[21] Gammel P L, Schneemeyer L F and Bishop D J 1991 *Phys. Rev. Lett.* **66** 953
[22] Koch R H, Foglietti V, Gallagher W J, Koren G, Gupta A and Fisher M P A 1989 *Phys. Rev. Lett.* **63** 1511
[23] Bates D M and Watts D G 1988 *Nonlinear Regression and its Applications* (New York: Wiley)
[24] Fisher M P A, Weichman P B, Grinstein G and Fisher D S 1989 *Phys. Rev.* B **40** 546
[25] Nelson D R and Vinokur V M 1992 *Phys. Rev. Lett.* **68** 2398
[26] Hwa T, Nelson D R and Vinokur V M 1993 *Phys. Rev.* B **48** 1167
[27] Nelson D R and Vinokur V M 1993 *Phys. Rev.* B **48** 13060